PROCEEDINGS OF SCIENCE

The IXPE view of GRB 221009A

Niccolò Di Lalla,[a,*] **Michela Negro,**[b,c,d] **Nicola Omodei,**[a] **Peter Veres,**[e,f] **Stefano Silvestri,**[g,h] **Alberto Manfreda**[g,i] **and Eric Burns**[l] **for the IXPE collaboration**

[a] *W. W. Hansen Experimental Physics Laboratory, Kavli Institute for Particle Astrophysics and Cosmology, Department of Physics and SLAC National Accelerator Laboratory, Stanford University, Stanford, CA 94305, USA*

[b] *University of Maryland, Baltimore County, Baltimore, MD 21250, USA*

[c] *NASA Goddard Space Flight Center, Greenbelt, MD 20771, USA*

[d] *Center for Research and Exploration in Space Science and Technology, NASA/GSFC, Greenbelt, MD 20771, USA*

[e] *Department of Space Science, University of Alabama, Huntsville, AL 35899, USA*

[f] *Center for Space Plasma and Aeronomic Research, University of Alabama, Huntsville, AL 35899, USA*

[g] *Istituto Nazionale di Fisica Nucleare, Sezione di Pisa, 56127 Pisa, Italy*

[h] *Università di Pisa, Dipartimento di Fisica Enrico Fermi, 56127 Pisa, Italy*

[i] *Istituto Nazionale di Fisica Nucleare, Sezione di Napoli, 80126 Napoli, Italy*

[l] *Department of Physics and Astronomy, Louisiana State University, Baton Rouge, LA 70803, USA*

E-mail: niccolo.dilalla@stanford.edu

GRB 221009A is an exceptionally bright gamma-ray burst (GRB) that reached Earth on October 9th, 2022 after traveling through the dust of the Milky Way. The Imaging X-ray Polarimetry Explorer (IXPE) pointed at GRB 221009A on October 11th and measured, for the first time, the 2-8 keV X-ray polarization of both a GRB afterglow and rings of dust-scattered photons which are echoes of the GRB prompt emission. We set upper limits to the polarization degree of the afterglow and the prompt emission of respectively 13.8% and 55% at a 99% confidence level, providing constraints on the jet opening angle of the GRB and other properties of the emitting region. In this contribution, I present on behalf on the IXPE Collaboration the results of the analysis and interpretation of the IXPE observation of GRB 221009A.

38th International Cosmic Ray Conference (ICRC2023)
26 July - 3 August, 2023
Nagoya, Japan

*Speaker

PoS(ICRC2023)870

1. Introduction

Gamma-Ray Bursts (GRBs) are among the most energetic events in the Universe. These events are characterized by a prompt gamma-ray emission, the most luminous phase of the burst, followed by a temporally decaying afterglow that can last for days or even years and is typically observed across the whole electromagnetic spectrum. Despite the detection of over 10,000 GRBs so far, our understanding of these events and the underlying physical processes is still limited [1]. Polarization measurements of GRBs can help to improve our knowledge by providing a unique observable to constrain the outflow composition and dynamics and to determine the structure of the magnetic fields in the jet as well as our viewing angle within its opening angle [2, 3]. Thus far, GRB polarization observations in the prompt phase have only occurred in the hard X-ray / soft gamma-ray band, reporting generally high polarization degrees, but never an unambiguous detection [4], while no observations of afterglow polarization have been reported so far at X-ray energies.

On October 9, 2022 an exceptionally bright long GRB outshone the rest of the high-energy sky. The first trigger was recorded in the gamma-ray band by the *Fermi* Gamma-ray Burst Monitor (GBM) at 13:16:59.988 UTC [5, 6], followed by many other instruments who soon reported their detection through the Gamma-Ray Coordinate Network (GCN) and The Astronomer's Telegram (ATEL). This event is by far the brightest ever recorded by any gamma-ray burst monitor at Earth and occurred close enough to the Galactic plane ($\sim$ 4 degrees) to form dust-scattered soft X-ray rings [7]. Such rings are in fact produced by X-rays from the extremely bright prompt emission efficiently scattered at small angles by interstellar dust grains in our Galaxy [8].

The Imaging X-ray Polarimetry Explorer (IXPE) is a space observatory with three identical telescopes designed to measure the polarization of astrophysical X-rays [9, 10]. Launched on 2021 December 9, IXPE is the result of an international collaboration between NASA and the Italian Space Agency (ASI), and it has been successfully operating since January 2022. IXPE measures polarization using the photo-electric effect of X-rays absorbed in the gas cell of a Gas Pixel Detector (GPD) [11]. On 2022 October 11 at 23:35:35.184 UTC IXPE started the observation of GRB 221009A in response to a Target of Opportunity request [12]. The observation ended on 2022 October 14 at 00:46:44.184 UTC with an effective exposure of 94,122 s. The content of this proceeding is based on the published research article [13] from the same authors.

2. IXPE Polarization Analysis

We analyze IXPE Level 2 processed data, which are publicly available on the HEASARC archive, combining the data collected by the three identical detector units (DUs). The count map of the observation is reported on the left side of Figure 1. As thoroughly discussed in [13], prior to the data analysis, we perform a background rejection procedure to remove a significant fraction of background events, mostly due to cosmic rays interacting in the sensitive area of the instrument. The residual cosmic-ray background component is then properly estimated via a dedicated Monte Carlo simulation using *ixpeobssim* [14] and based on previous IXPE observations. The correct modeling of such a component is indeed particularly relevant to study the fainter extended emission of the dust-scattering rings.

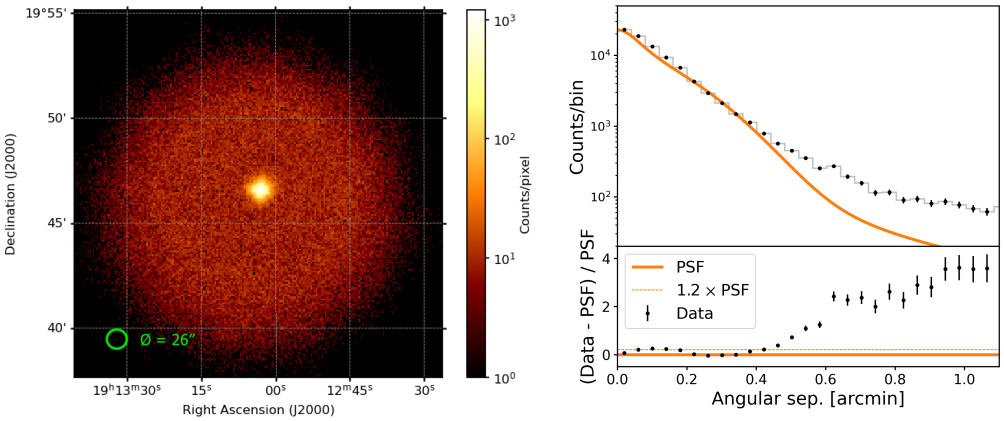

Figure 1: Left: Count map of the IXPE observation of GRB 221009A with superimposed the typical IXPE PSF. Right: Background-rejected radial profile around the core emission for DU1; as shown in the lower panel, the source profile starts deviating more than 20% from the instrumental PSF at around 0.43 arcmin. The equivalent plots for DU2 and DU3 are not reported here as they carry the same information. Images taken from [13].

Typically, for IXPE observations, the polarization information is extracted via two types of analyses: a polarimetric analysis and a spectro-polarimetric analysis. For the former, we use the *xpbin* routine of *ixpeobssim* (PCUBE algorithm), which calculates the polarization degree (PD) and polarization angle (PA) with associated errors from the Q/I and U/I parameters following the recipe of [15]. The spectro-polarimetric analysis instead consists in a joint fit of the I, Q and U spectra and therefore also accounts for the shape of the intensity spectrum. To this purpose, we made use of the publicly available Multi-Mission Maximum Likelihood (`3ML`) framework [16].

The time-integrated radial profile reveals inconsistency with the expectation from a point-like source, showing a profile that progressively deviates from the expected instrument point spread function (PSF) profile (Figure 1, right panel). In particular, as shown below, two excesses are visible as rings around the bright core emission and are associated with dust-scattering halos. Hereafter, we refer to the central region as the *core*, while the inner and the outer rings are denoted r_1 and r_2, respectively. In the next subsections we will illustrate the data analyses and results for these different regions.

2.1 The Core

We start with the analysis of the *core*, which arises from the burst afterglow. We select the region as a disc centered on the brightest pixel of the IXPE image and radius of 26 arcsec (0.43 arcmin). Beyond this radius, the radial profile of the emission deviates from the PSF of the instrument by more than 20%, as shown in Figure 1 (right panel), due to the unresolved emission of dust-scattered X-rays.

Through the PCUBE analysis, we find an unconstrained polarization in the 2–8 keV energy range and derive a 99% C.L. upper limit of 16.1%. No evolution with time or energy is observed. For the spectro-polarimetric analysis we model the observed spectrum with an absorbed power law decreasing in energy and we find a best-fit power-law index of $\Gamma_{core} = 1.98 \pm 0.03$, in agreement

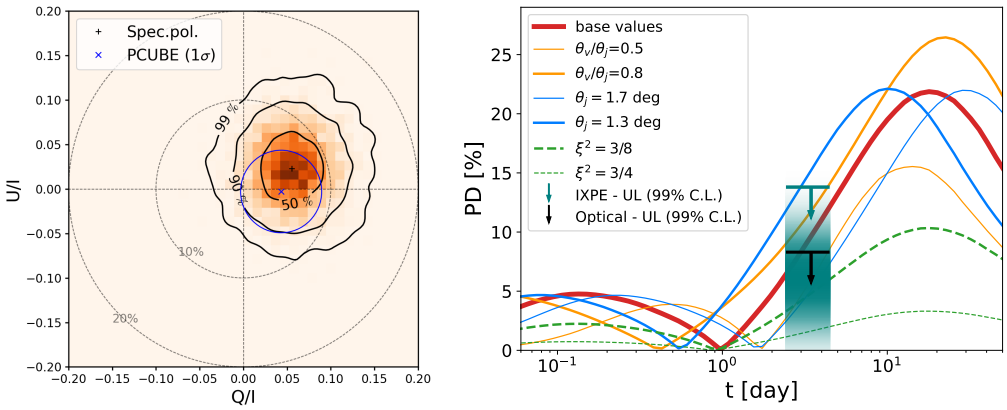

Figure 2: Left: Q/I versus U/I plot; in orange we show the distribution resulting from the spectro-polarimetric analysis and the 50%, 90% and 99% C.L. contours in black. The blue cross and circle show the PCUBE analysis result and the related 1 sigma error. Right: Polarization lightcurves using a set of base parameter values. We show the effect of changing the θ_v/θ_j ratio, the jet opening angle, θ_j and the magnetic field ratio, ξ. The IXPE upper limits are shown in teal, while the black upper limit marks the upper limit of the contemporaneous optical observation at the Nordic Optical Telescope [17]. The shaded band shows a Gaussian modulation centered on the PD (darker shade) and width equal to the one sigma uncertainty on the PD (from the spectropolarimetric fit). See [13] for additional details.

with expectations from a late afterglow emission. The left panel of Figure 2 shows the Q/I versus U/I distribution of the *core* emission. The polarization results found in this case are slightly more constraining than, but still in agreement with, the PCUBE analysis with a PD = 6.1 ± 3.0%, which we use to set an upper limit to the polarization degree (1D distribution) of 13.8% at 99% C.L..

For an uniform (top-hat) jet structure with no sideways expansion, significant polarization arises from the break in symmetry of the visible surface. This surface is typically an annulus when projected to the plane of the sky. As the annulus grows, it encompasses a progressively larger fraction of the jet surface. Eventually, for an off-axis observer, the annulus will grow beyond the size of the jet on one side, while still collecting emission from the opposite side, resulting in net polarization. The polarization lightcurve exhibits the typical two-bump structure [18–20], in which the minimum between the bumps is broadly associated with the jet break time and marks the rotation of the polarization angle by 90 degrees. Our models, presented in Figure 2 (right panel), are constructed so that the PD zero point between the two bumps is at $\approx$ 1 day, to match the estimated jet break time [21]. The evolution of the polarization as a function of time depends strongly on a variety of parameters, namely the jet opening angle θ_j, the ratio between the viewing angle and the jet opening angle θ_v/θ_j and the ratio of the magnetic field strength ξ in the directions parallel and perpendicular to the shock normal. All presented models in the right panel of Figure 2, except the low jet opening angle, are consistent with the upper limit. Taking the PD = 6.1 ± 3.0% at face value, models with jet opening angle $\theta_j < 1.5$ deg (while keeping all other base values fixed) are disfavored. Similarly, models with $\theta_v/\theta_j > 2/3$ tend to overpredict the IXPE measurement. Assuming a magnetic field ratio ξ closer to 1 simply scales down the PD. In principle, any model that overpredicts the observations can be made consistent by appropriate choice of ξ. The IXPE measurement, considering the base values, favors cases where $\xi^2 \lesssim 1/2$.

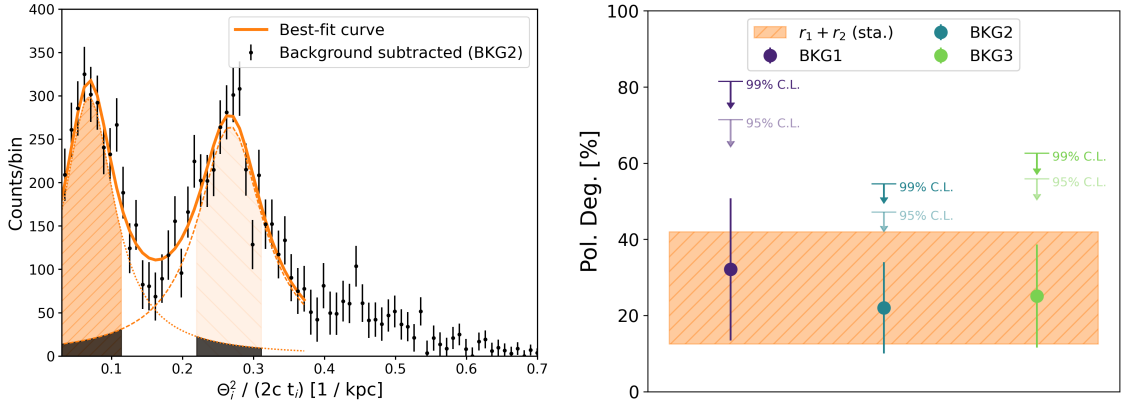

Figure 3: Left: Background subtracted distribution of the angular distance θ_i from the center of the core rescaled with the time since the GRB trigger, showing the prominent contribution from the two rings. Right: Results of the spectro-polarimetric fit for the PD assuming different background templates. The orange band is centered on the average of the best-fit values weighted by their uncertainties, and has a width representative of the mean relative statistical error. Images taken from [13].

2.2 The Rings

As mentioned in the introduction, the observed rings are the result of a known effect involving Galactic dust along the line-of-sight of a bright transient event. A fraction of the photons emitted in the prompt phase of the GRB are scattered by dust clouds in the Milky Way. Those scattered inwards towards the line of sight arrive at Earth after traveling a longer path length with respect to the unscattered ones and are thus echoes of the prompt emission. Being produced by a short transient event, the rings expand radially in time, as photons with different scattering angles travel different path lengths. In order to study the radial evolution of the rings and correctly select prompt, scattered photons as the rings expand, we developed a time-dependent selection method inspired by the procedure described in [22] and discussed in details in [13].

To avoid contamination from the dominant *core* (afterglow) emission, we select events at radial distances larger than 0.85 arcmin from the center. The left panel of Figure 3 shows the background-subtracted event distribution as a function of $\theta_i^2/(2ct_i)$, where θ_i is the angular distance (in arcsec) from the center of the core and t_i is the time passed since the GRB trigger time. The contribution of the two rings is clearly visible. We fit the distribution around the peaks with the sum of two Lorentzian functions and we define the event selection cut so that the area under each best-fit Lorentzian between R^i_{min} and R^i_{max} (orange areas in the plot), where $i = 1, 2$ denotes r_1 and r_2 respectively, is at least a factor of 20 larger than the area under the other Lorentzian in the same range (gray areas in the plot). This ensures a negligible contamination from the emission of one ring onto the other.

Similar to what done in the *core* analysis, we proceed with the PCUBE polarization analysis in the 2–8 keV energy band. The observed spectra of the two rings are expected to be different because they are generated from the same prompt emission scattered at different angles. For this reason, combining the two ring selections into one single PCUBE analysis would be inaccurate. We find a $PD_{r_1} = 19.6 \pm 8.7\%$ and $PD_{r_2} = 17.2 \pm 8.8\%$, in agreement with each other. The

spectro-polarimetric fit enables a proper combination of the rings selections and can therefore give a more accurate estimation of the underlying polarization. The phenomenological model we define to describe the rings emission allows for the spectral parameters of the rings to be different while sharing common polarization parameters. The spectra of both rings are modeled as absorbed simple power laws, while we assume constant polarization parameters. As opposed to the PCUBE analysis, we perform here the subtraction of the background spectrum, testing different background templates as described in [13]. We find that the PD value and uncertainty depend upon the assumed background. The low-statistic regime of the ring data, indeed, causes the measurement to be strongly affected by small changes of the subtracted background. The statistical-error-weighted average is $(27.2 \pm 15.1\ (\text{sta.}) \pm 4.0\ (\text{sys.}))\%$, where the statistical error is the average among the statistical uncertainties obtained assuming different backgrounds, and the systematic uncertainty is given by the variation of the best-fit value assuming different backgrounds. The right panel of Figure 3 shows the results for the different background subtractions. The 1D 99% C.L. upper limit on the PD varies between 54.6% and 81.5%, depending on the assumed background.

A high polarization degree (PD $\gtrsim$ 20%) in the prompt phase, when viewing the jet at angles smaller than the opening angle, $\theta_v < \theta_j$, can be achieved by synchrotron emission in an ordered, toroidal magnetic field configuration [23]. Alternatively, high polarization can be achieved by random magnetic fields or Compton drag models, in a geometry where we are viewing the jet close to its edge, $\theta_j \lesssim \theta_v < \theta_j + 1/\Gamma_j$ [24]. This scenario would result in a very early jet break and potentially high PD in the afterglow, which is disfavored by the observations. Considering then the ordered synchrotron scenario, we can estimate the polarization degree integrated over the duration of the prompt emission. The PD mainly depends on the photon index, the viewing angle, and the product of the jet opening angle and the Lorentz factor, $y_j = (\theta_j \Gamma_j)^2$. Using $\Gamma_j = 700$ [25], $\theta_j = 1.5$ deg, $\theta_v = \frac{2}{3}\theta_j$ and a photon index ranging between 0.62 and 1.25 [13], we obtain 16% and 36%, respectively, which is consistent with the measured upper limits.

3. Conclusions

IXPE observed GRB 221009A from October 11 at 23:35:35 UTC to October 14 at 00:46:44 UTC for an effective exposure to the target of 94,122 s. The imaging capability of the instrument revealed the presence of a bright core emission, associated with the GRB afterglow, and the extended emission of two expanding dust-scattering halo rings. Such emission is an echo of the GRB prompt emission and therefore carries information about the latter. We studied the linear polarization properties of the afterglow emission, and derived an upper limit on the polarization degree of 13.8% at the 99% C.L. The observed upper limit on the polarization degree favors a jet opening angle to be wider than 1.5 degrees, and a viewing angle wider than 2/3 of the jet opening angle. Also, scenarios with an equal magnetic field strength in the two directions parallel and perpendicular to the shock normal seem to be disfavored. The polarization analysis of the combined dust-scattering rings revealed a non-significant polarization degree around $(27.2 \pm 15.1(\text{sta.}) \pm 4.0(\text{sys.}))\%$ with 99% C.L. upper limit ranging between 54.6% and 81.5% depending on the assumed background. Considering a scenario involving toroidal, ordered magnetic fields when the viewing angle is smaller than the jet opening angle, predicts high polarization degree up to 36%, compatible with the observed upper limits.

References

[1] B. Zhang, *The physics of gamma-ray bursts*, Cambridge University Press (2018).

[2] R. Gill, M. Kole and J. Granot, *GRB Polarization: A Unique Probe of GRB Physics*, *Galaxies* **9** (2021) 82 [2109.03286].

[3] E.M. Rossi, D. Lazzati, J.D. Salmonson and G. Ghisellini, *The polarization of afterglow emission reveals γ-ray bursts jet structure*, *MNRAS* **354** (2004) 86.

[4] M.L. McConnell, *High energy polarimetry of prompt GRB emission*, *NewAR* **76** (2017) 1 [1611.06579].

[5] P. Veres, E. Burns, E. Bissaldi, S. Lesage, O. Roberts and Fermi GBM Team, *GRB 221009A: Fermi GBM detection of an extraordinarily bright GRB*, *GRB Coordinates Network* **32636** (2022) 1.

[6] S. Lesage, P. Veres, O.J. Roberts, E. Burns, E. Bissaldi and Fermi GBM Team, *GRB 221009A: Fermi GBM observation*, *GRB Coordinates Network* **32642** (2022) 1.

[7] A. Tiengo, F. Pintore, S. Mereghetti, R. Salvaterra and a larger Collaboration, *Swift/XRT discovery of multiple dust-scattering X-ray rings around GRB 221009A*, *GRB Coordinates Network* **32680** (2022) 1.

[8] J. Miralda-Escudé, *Small-Angle Scattering of X-Rays from Extragalactic Sources by Dust in Intervening Galaxies*, *ApJ* **512** (1999) 21 [astro-ph/9808277].

[9] S.L. O'Dell, P. Attinà, L. Baldini, M. Barbanera, W.H. Baumgartner, R. Bellazzini et al., *The Imaging X-Ray Polarimetry Explorer (IXPE): technical overview II*, in *UV, X-Ray, and Gamma-Ray Space Instrumentation for Astronomy XXI*, O.H. Siegmund, ed., vol. 11118 of *Society of Photo-Optical Instrumentation Engineers (SPIE) Conference Series*, p. 111180V, Sept., 2019, DOI.

[10] P. Soffitta, P. Attinà, L. Baldini, M. Barbanera, W.H. Baumgartner, R. Bellazzini et al., *The Imaging X-ray Polarimetry Explorer (IXPE): technical overview III*, in *Society of Photo-Optical Instrumentation Engineers (SPIE) Conference Series*, vol. 11444 of *Society of Photo-Optical Instrumentation Engineers (SPIE) Conference Series*, p. 1144462, Dec., 2020, DOI.

[11] R. Bellazzini, F. Angelini, L. Baldini, F. Bitti, A. Brez, F. Cavalca et al., *Gas pixel detectors for X-ray polarimetry applications*, *Nuclear Instruments and Methods in Physics Research A* **560** (2006) 425 [astro-ph/0512242].

[12] M. Negro, A. Manfreda, N. Omodei and IXPE Collaboration, *GRB 221009A: planned observation with the Imaging X-ray Polarimetry Explorer (IXPE)*, *GRB Coordinates Network* **32690** (2022) 1.

[13] M. Negro, N. Di Lalla, N. Omodei, P. Veres, S. Silvestri, A. Manfreda et al., *The IXPE View of GRB 221009A*, *ApJL* **946** (2023) L21 [2301.01798].

[14] L. Baldini, N. Bucciantini, N.D. Lalla, S. Ehlert, A. Manfreda, M. Negro et al., *ixpeobssim: A simulation and analysis framework for the imaging X-ray polarimetry explorer*, *SoftwareX* **19** (2022) 101194 [2203.06384].

[15] F. Kislat, B. Clark, M. Beilicke and H. Krawczynski, *Analyzing the data from x-ray polarimeters with stokes parameters*, *Astroparticle Physics* **68** (2015) 45.

[16] G. Vianello, R.J. Lauer, P. Younk, L. Tibaldo, J.M. Burgess, H. Ayala et al., *The Multi-Mission Maximum Likelihood framework (3ML)*, *arXiv e-prints* (2015) arXiv:1507.08343 [1507.08343].

[17] E. Lindfors, K. Nilsson, I. Liodakis, A. Kasikov and I. Negueruela, *Optical polarization observation of GRB 221009A*, *GRB Coordinates Network* **32995** (2022) 1.

[18] G. Ghisellini and D. Lazzati, *Polarization light curves and position angle variation of beamed gamma-ray bursts*, *MNRAS* **309** (1999) L7 [astro-ph/9906471].

[19] R. Sari, *Linear Polarization and Proper Motion in the Afterglow of Beamed Gamma-Ray Bursts*, *ApJL* **524** (1999) L43 [astro-ph/9906503].

[20] J. Shimoda and K. Toma, *Multi-wave band Synchrotron Polarization of Gamma-Ray Burst Afterglows*, *ApJ* **913** (2021) 58 [2005.03710].

[21] P. D'Avanzo, M. Ferro, R. Brivio, M.G. Bernardini, D. Fugazza, S. Campana et al., *GRB 221009A: continued REM optical/NIR observations and evidence for an achromatic steepening in the afterglow light curve*, *GRB Coordinates Network* **32755** (2022) 1.

[22] A. Tiengo and S. Mereghetti, *Dust-scattered X-ray halos around gamma-ray bursts: GRB 031203 revisited and the new case of GRB 050713A*, *A&A* **449** (2006) 203 [astro-ph/0511186].

[23] K. Toma, T. Sakamoto, B. Zhang, J.E. Hill, M.L. McConnell, P.F. Bloser et al., *Statistical Properties of Gamma-Ray Burst Polarization*, *ApJ* **698** (2009) 1042 [0812.2483].

[24] J. Granot, *The Most Probable Cause for the High Gamma-Ray Polarization in GRB 021206*, *ApJL* **596** (2003) L17 [astro-ph/0306322].

[25] R.-Y. Liu, H.-M. Zhang and X.-Y. Wang, *Constraints on the Model of Gamma-ray Bursts and Implications from GRB 221009A: GeV gamma rays v.s. High-energy Neutrinos*, *arXiv e-prints* (2022) arXiv:2211.14200 [2211.14200].